INTERNATIONAL JOURNAL OF INTEGRATED ENGINEERING
ISSN: 2229-838X e-ISSN: 2600-7916

IJIE

Vol. 16 No. 6 (2024) 285-293
https://publisher.uthm.edu.my/ojs/index.php/ijie

Optimizing Bionic Prosthetic Finger 3D Topology Design and Comprehensive Testing of Fully Compliant Mechanisms

Shrishail B Sollapur[1]*, Mangesh Y Dakhole[2], Shubham R. Suryawanshi[3], Nitisha Achmelwar[4], Vishnu Vijay Kumar[1]*, Suriani Abu Bakar[5,6]

[1] *Department of IIAEM, Faculty of Engineering and Technology, JAIN (Deemed to be University) Bengaluru, Karnataka 560069, INDIA*
[2] *Department of Mechanical Engineering, PES's Modern College of Engineering, Savitribai Phule Pune University, Pune-411005, Maharashtra, INDIA*
[3] *Department of Mechanical Engineering, MET's Institute of Engineering, Nashik, SPPU, Pune, INDIA*
[4] *Department of Mechanical Engineering, DJ SANGHVI College of Engineering, Mumbai, Maharashtra 410206, INDIA*
[5] *Nanotechnology Research Centre, Faculty of Science and Mathematics, Universiti Pendidikan Sultan Idris, 35900 Tanjung Malim, Perak, MALAYSIA*
[6] *Department of Physics, Faculty of Science and Mathematics, Universiti Pendidikan Sultan Idris, 35900 Tanjung Malim, Perak, MALAYSIA*

*Corresponding Author: shrishail.sollapur@gmail.com, vishnu.vijay@u.nus.edu
DOI: https://doi.org/10.30880/ijie.2024.16.06.027

Article Info

Received: 13 June 2024
Accepted: 24 November 2024
Available online: 29 December 2024

Keywords

3D topology, flexible, prosthetic human finger, FEM, MATLAB

Abstract

Compliant mechanisms, with their cohesive structure and adaptable motion, are well-suited for creating prosthetic digits that closely mimic the functionality of human fingers. However, designing flexible prosthetic fingers is challenging because traditional assumptions based on rigid-link systems do not translate well. This study presents an innovative 3D structure optimization approach for designing prosthetic fingers that are compatible with biological systems. The suggested method, carried out in MATLAB, allows for quick production of these fingers through the use of selective laser sintering technology. A design example is presented, utilizing load testing and finite element simulations to effectively validate the realized finger's bending capability, clarifying the framework's implementation. The refined fingers demonstrate promising potential for integration into prosthetic hands in future endeavors, enabling intricate, gripping actions akin to the human hand.

1. Introduction

Accidents or planned operations to stop the spread of infections frequently lead to hand amputations. Various prosthetic hands and fingers have been designed to restore hand function [1-3]. Rigid-link systems, such as the DLR Hand II or the Delft Cylinder Hand, which provide stability and robustness, are typically used in prosthetic fingers. A cosmetic prosthetic hand was produced using a 3D scanner as part of some studies on 3D printing [4-6]. However, rigid-link devices have drawbacks, such as difficult installation and upkeep needs. These constraints are addressed by compliant methods, which rely on elastic deformation [7-8]. For instance, a cable-driven continuum-based hand and a tendon-driven compliant thumb [9-11] mimic natural hand characteristics.

Nevertheless, portraying flexible fingers is difficult because of the consequences of these processes. To create compliant fingertips, researchers have suggested topology optimization [12-14] and 3D printing [15-16]. This research presents a unique design approach for compliant prosthetic fingers with 3D topology optimization motivated by biological evolution. Realized fingers have flexible bionic shapes as shown in Figure 1[17-19]. The outline is implemented in MATLAB [20-21], enhancing the performance of the designs by integrating with 3D printing and optimizing the efficiency of the code.

Through this innovative methodology, optimized compliant prosthetic fingers can be rapidly manufactured, addressing the shortcomings of traditional rigid-link systems while closely replicating the intricate motions and gripping abilities of the human hand. As these techniques continue to evolve, they have the potential to significantly improve the lives of individuals with hand amputations by providing prosthetics that more closely mimic the capabilities of natural hands.

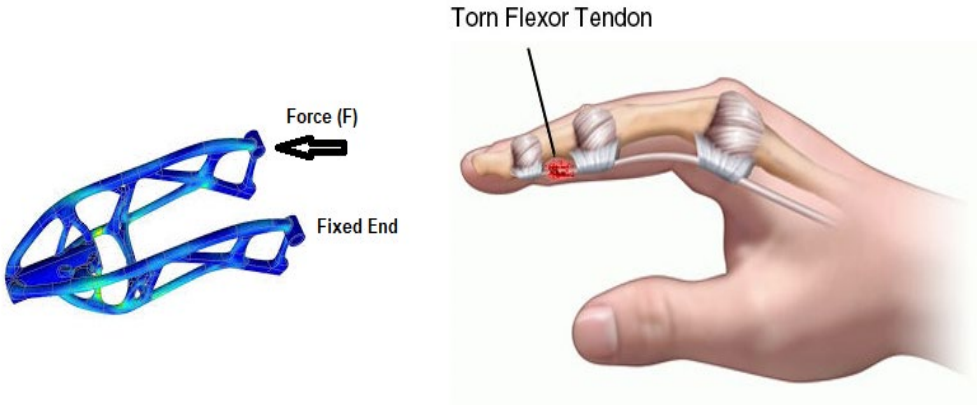

Fig. 1 *Bionic vs. biological finger mechanisms (a) 3D-optimized prosthetic finger; (b) Human finger tendon system*

2. Methodology

2.1 Design Process

The recommended design framework, detailed in Algorithm 1, begins by creating a 3D design domain for the prosthetic finger as shown in Figure 2, using a cuboid mesh of $n_x * n_y * n_z$ cubic elements. Boundary conditions, including actuation forces and bending orientations, are then established to define the expected objective function f(x) for the prosthetic finger.

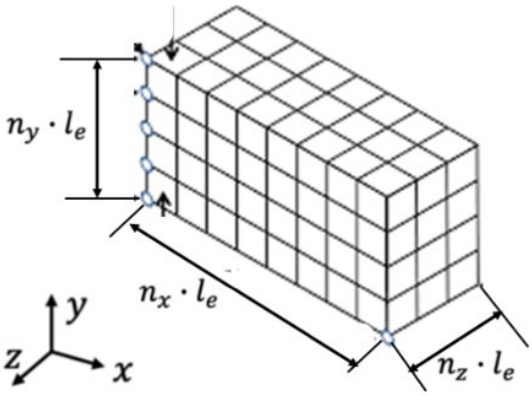

Fig. 2 *3D cubic element mesh model*

At its heart, the process of creating a form involves 3D topology optimization, which repeatedly carries out 3D finite element analysis to assess a set of predetermined goals. In every step, the distribution x, which shows the normalized density of materials over the design area, is gradually modified through a method of updating. After the optimization reaches a point of convergence, further postprocessing methods are used, leading to the creation of a working 3D-printed prosthetic finger. This approach integrates advanced computational methods with additive manufacturing to create optimized prosthetic fingers that balance performance and manufacturability.

Int. Journal of Integrated Engineering Vol. 16 No. 6 (2024) p. 285-293

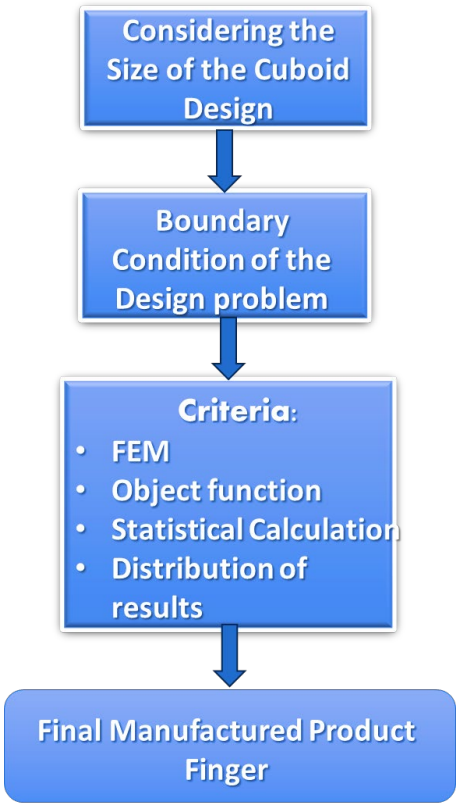

Algorithm 1 *The design framework for the 3D topology optimization workflow*

2.2 The 3D Topology Optimization Method Algorithm is as Follows

The main goal of the suggested 3D topology optimization method is to explore a roughly solid-vacuum density distribution x across the 3D design space, with the goal of maximizing the movement of a selected output point Pout. To create the voxel model x, a MATLAB matrix with size (n_x, n_y, n_z) is used. The following is how the goal function is stated:

$$Max(x) = f(x) = L^T \times U = u_{out} \qquad (1)$$

$$\sum_{e=01}^{N} v_e \times x_e \leq V_0 \times c \qquad (2)$$

$$E_e = E_0 \times x_e^p, 0 < x_e \leq 1 \qquad (3)$$

In this context, U represents the displacement vector that encompasses all the nodes within the design area, while L serves as a vector that separates the output displacement from U. The magnitude of the resulting finger is limited by the volume fraction factor, represented by the variable c. A 3D finite element analysis (FEA) employs the global stiffness matrix K and the global load vector F to calculate U. However, x is not directly linked to the stiffness matrix K, we add x into FEA using $E_e = E_0 \times x_e^p$, where E0 represents the material's elastic modulus at full density and p is a penalty parameter [22]. The optimization problem is solved iteratively by updating x. The associated updating process may be described using Algorithm 2. In the above procedure, m denotes the step-by-step preset limit of movement for x_e, and δ denotes a damping factor. To preserve the numerical stability of x, these two parameters are introduced.

Once the necessary convergence criteria are satisfied, a distribution of x that is very nearly solid vacuum (1-0) is achieved. The marching cubes method [23] is employed to generate an iso-surface from the x distribution in the postprocessing phase, thereby producing a 3D representation of the actual prosthetic finger. In the end, the computed finger model may be used for 3D printing, allowing the development of prototypes for testing and assessment.

3. Illustrative Design Model

In this part, the creation and examination of a prosthetic finger designed to be compatible with bionic technology are shown to demonstrate the application and assessment of the suggested framework for design.

3.1 Analysis and Manufacture of a Finger

Figure 3 shows the design specifications for the compliant finger in the context of creating a prosthetic finger. Notably, the design domain is cuboid with 100 × 25 × 15 cubic pieces, each with a size of 0.6 mm. The design process for the proposed prosthetic finger leverages symmetry to enhance efficiency. As shown in Figure 3, the correct side of the design area was identified as the symmetry line. This strategic choice allowed for the synthesis of only half of the finger within the initial design domain, with all boundary conditions mirrored accordingly. By exploiting this symmetrical property, the computational requirements were significantly reduced, streamlining the overall design and optimization process without compromising the integrity of the final prosthetic finger model.

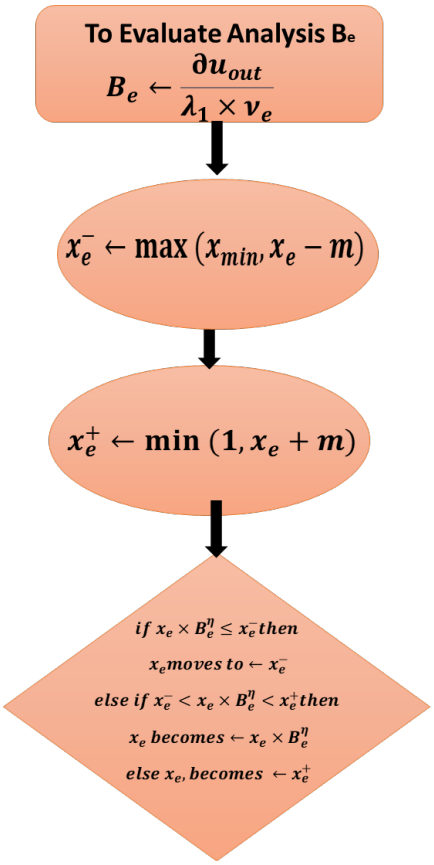

Algorithm 2 *The iterative process for updating variable x follows this algorithm*

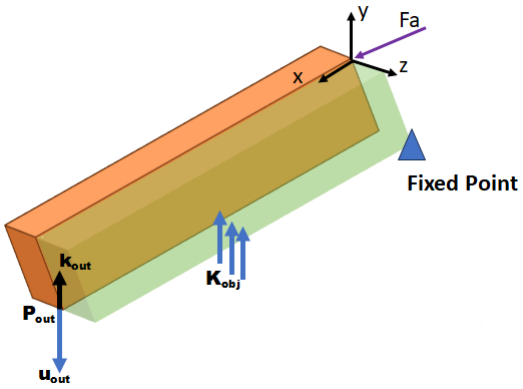

Fig. 3 *Prosthetic finger design challenge*

Int. Journal of Integrated Engineering Vol. 16 No. 6 (2024) p. 285-293

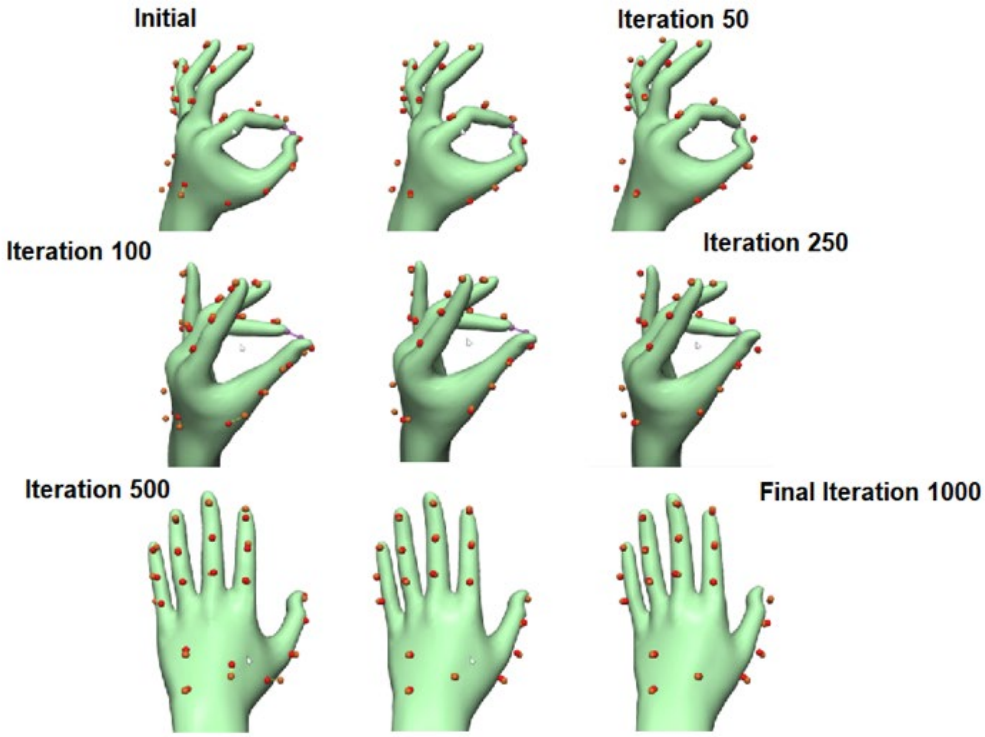

Fig. 4 *3D topology optimization: x progression over 1000 iterations*

To model how the compliant finger would act, a force based on movement (F_a) was introduced into the test area, measured in millimeters (mm). This force's change in position is shown by the blue line in the illustration (u_{out}). To mimic the friction experienced while holding objects with the finger joint and the point at the end, rubber springs (k_{obj} = 0.85 N/mm and k_{out} = 0.7 N/mm) were placed at the middle and end points in the x-direction. The green region outlines the point at which the structure is at rest. The compliant finger was created using selective laser melting (SLM), a process using polyamide, which behaves elastically in a linear way. The physical properties of the polyamide were chosen based on its characteristics, including the Young's modulus (E_0) in 1700 MPa and the Poisson's ratio (v) at 0.28. Figure 4 shows how the displacement changes with time, reflecting the structure's development towards its completion.

The objective function converged after 1000 iterations, with the maximum U_{out} reaching 12.014 mm, as depicted in Figure 5. Post-processing resulted in a symmetrical and cohesive bionic finger, shown in Figure 6a. To evaluate its flexibility, the finger was materialized through SLS. The prototype, presented in Figure 6b, incorporated a flange for secure attachment and subsequent actuation by a servo motor.

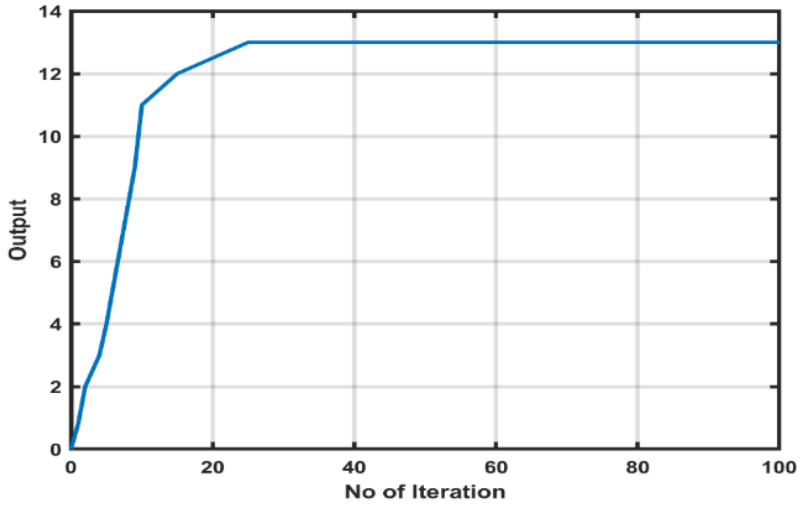

Fig. 5 *Iteration process*

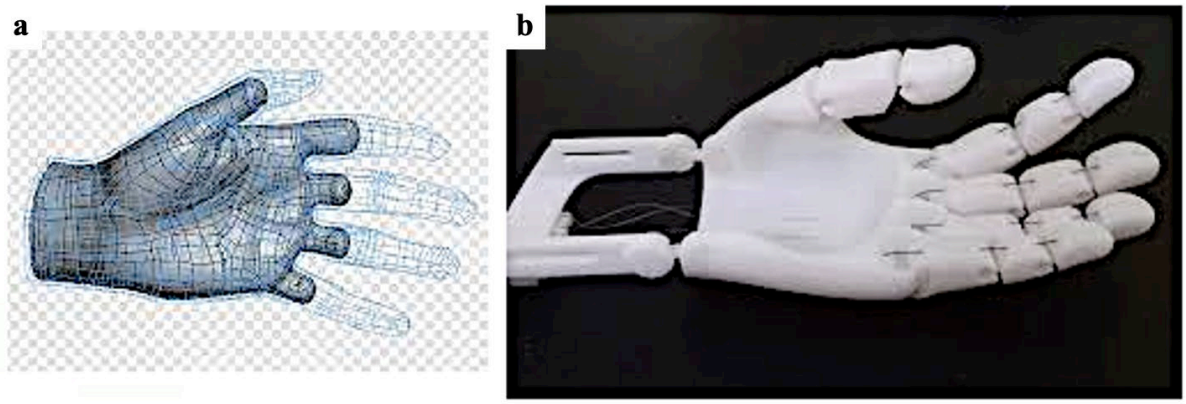

Fig. 6 *Artificial finger: Surface model and SLS prototype*

3.2 Finite Element Analysis (FEA) Simulation of an Enhanced Finger Model

A large-displacement in-depth analysis of the stress distribution within an actual bionic finger during bending was performed using finite element analysis (FEA) [24-25]. The bulk of the deformations and stress concentrations are uniformly distributed in the second half of the finger, as seen from an analysis of the simulation results displayed in Figure 7a. This distribution significantly contributes to the decrease in mechanical fatigue. The twisted form was further confirmed by the bent prototype, as shown in Figure 7b.

4. Experimental Load Setup

A test involving a payload was carried out to find out the duration of a manufactured finger's durability when it encounters an object. The compliant finger was attached to a base on the experimental apparatus depicted in Figure 8, enabling it to be flexed by a servo motor. Throughout the payload test, a system operated by sensors provided a steady force Ft at the tip of the finger as it was flexed by the force applied. To simulate the usual force applied by a human finger upon contact, F_t was set at 3 N. To determine how the touching force influenced the bending performance, the displacement din at the actuation point and the vertical displacement d_{out} at the fingertip were both measured. For comparison, these measurements were also made without any application of contact force.

Figure 9 depicts the outcomes of the experiment. Notably, Δd_{out} increases in an almost linear manner with Δd_{in}. In cases where no touch (star curve blue) and touch (plus curve red) were involved, the most significant change in Δd_{out} was approximately 2.8 mm, as observed at $\Delta d_{in} = 0mm$. This minimal discrepancy in Δd_{out} highlights the stability and resilience of the fabricated compliant finger when subjected to normal touching forces.

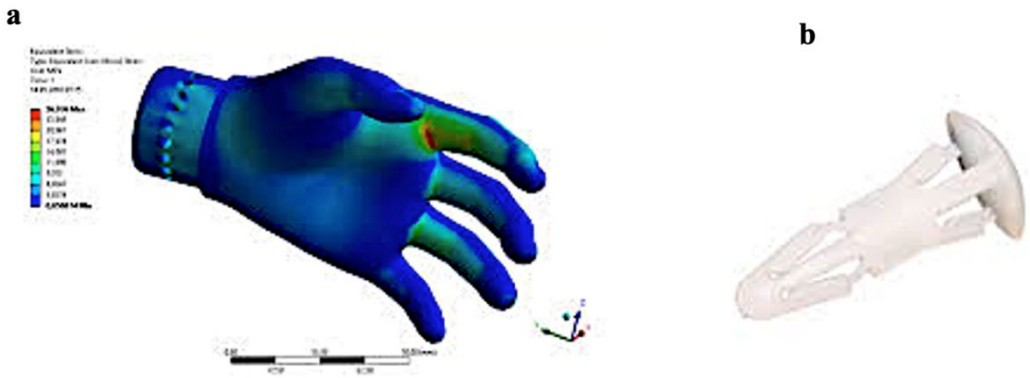

Fig. 7 *Finger flexion: physical bending and FE stress analysis (7 mm displacement)*

Int. Journal of Integrated Engineering Vol. 16 No. 6 (2024) p. 285-293

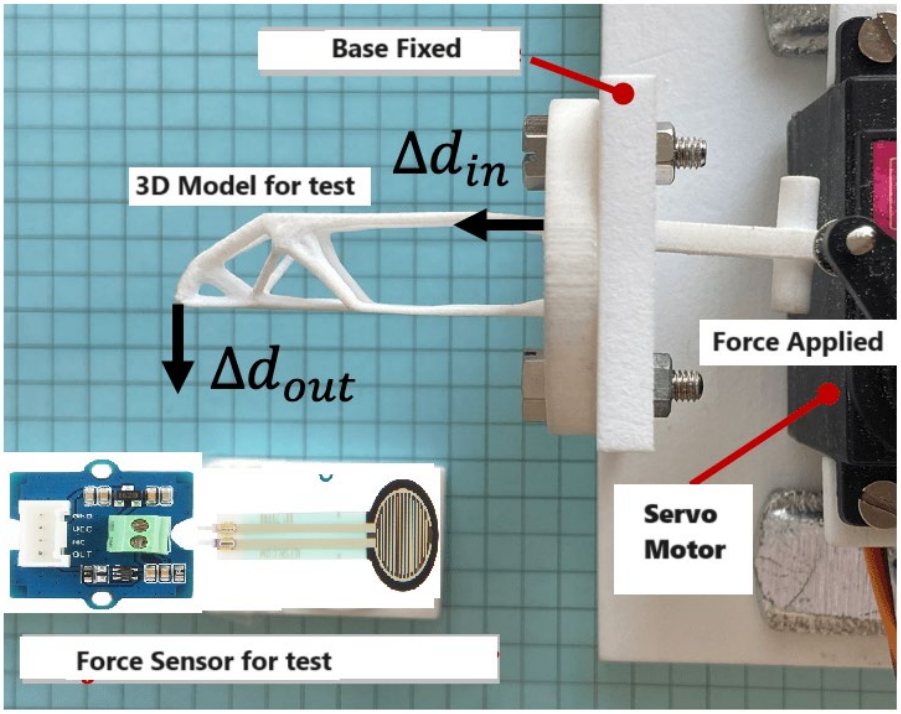

Fig. 8 *Payload test setup: Force sensor measuring constant touch force*

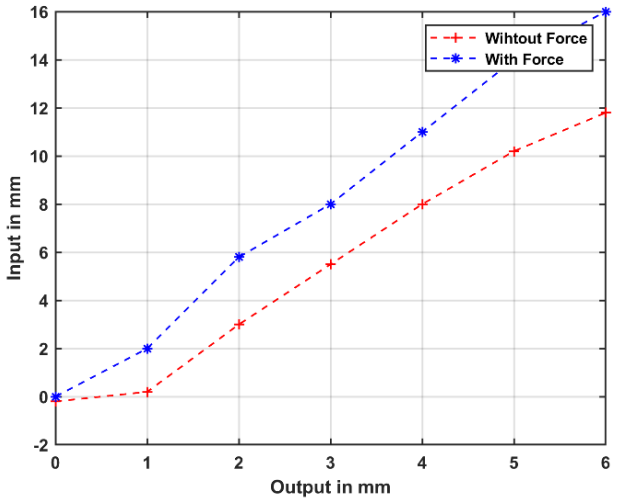

Fig. 9 *Fingertip displacement (d_{out}) vs. input displacement (d_{in}), with and without F_t*

5. Conclusion

This paper presents a design framework that employs 3D topology optimization to develop bionic prosthetic fingers. Building upon our previous research on 2D topology optimization for synthesis, we have expanded the approach to three dimensions. To validate the practicality of this method, we conducted payload tests and finite element simulations. The outcomes effectively showed the flexibility of the actual compliant finger. Moving forward, we plan to extend this framework to create compliant fingers in various sizes. Our goal is to integrate these custom-designed fingers into a prosthetic hand, enabling the execution of complex gripping motions. This work represents a significant step towards more functional and biomimetic prosthetic hand designs.

Acknowledgement

We extend our sincere gratitude to the anonymous reviewers for their valuable feedback and insightful suggestions, which significantly contributed to improving the quality of this manuscript.

Conflict of Interest

Authors declare that there is no conflict of interests regarding the publication of the paper.

Author Contribution

All authors contributed equally to this work.

Data Availability

The data underlying this study will be made available upon request.

References

[1] Imbinto, C. Peccia, M. Controzzi, A. G. Cutti, A. Davalli, R. Sacchetti, and C. Cipriani, "Treatment of the partial hand amputation: An engineering perspective," IEEE Reviews in Biomedical Engineering, vol. 9, pp. 32–48, 2016.
[2] T. Murayama ,K. Oono, M. Tada, T. Eguchi, and M. Nagami, "Computer aided design and fabrication of finger prosthesis," J. Biomed. Sci. Eng., vol. 8, no. 2, pp. 98–103, 2015.
[3] P. F. Pasquina, M. Evangelista, A. J. Carvalho, J. Lockhart, S. Griffin, G. Nanos, and D. Hankin, "First-in-man demonstration of a fully implanted myoelectric sensors system to control an advanced electromechanical prosthetic hand," J. Neurosci. Methods, vol. 244, pp. 85–93, 2015.
[4] F.Z. Akbarzadeh, M. Sarraf, E.R. Ghomi, V.V. Kumar, M. Salehi, S. Ramakrishna, S. Bae, A state-of-the-art review on recent advances in the fabrication and characteristics of magnesium-based alloys in biomedical applications, Journal of Magnesium and Alloys, (2024). https://doi.org/10.1016/j.jma.2024.06.015
[5] C. Borst, M. Fischer, S. Haidacher, H. Liu, and G. Hirzinger, "Dlr hand ii: experiments and experience with an anthropomorphic hand," in 2003 IEEE International Conference on Robotics and Automation (Cat. No.03CH37422), vol. 1, pp. 702–707 vol.1, 2003.
[6] Shinde, Tarang, et al. "Fatigue analysis of alloy wheel using cornering fatigue test and its weight optimization." Materials Today: Proceedings 62 (2022): 1470-1474. https://doi.org/10.1016/j.matpr.2022.02.023
[7] G. Smit, D. H. Plettenburg, and F. C. T. van der Helm, "The lightweight delft cylinder hand: First multii-articulating hand that meets the basic user requirements," IEEE Transactions on Neural Systems and Rehabilitation Engineering, vol. 23, no. 3, pp. 431–440, 2015.
[8] M. Yoshikawa, R. Sato, T. Higashihara, T. Ogasawara, and N. Kawashima, "Rehand: Realistic electric prosthetic hand created with a 3d printer," in 2015 37th Annual International Conference of the IEEE Engineering in Medicine and Biology Society (EMBC), pp. 2470–2473, 2015.
[9] Sharath, P.C., Waghmare, P. (2024). Applications of Additive Manufacturing in Biomedical and Sports Industry. In: Rajendrachari, S. (eds) Practical Implementations of Additive Manufacturing Technologies. Materials Horizons: From Nature to Nanomaterials. Springer, Singapore. https://doi.org/10.1007/978-981-99-5949-5_13
[10] Chate, Ganesh R., et al. "Ceramic material coatings: emerging future applications." Advanced Ceramic Coatings for Emerging Applications. Elsevier, 2023. 3-17. https://doi.org/10.1016/B978-0-323-99624-2.00007-3
[11] S. Kolluru, A. Thakur, D. Tamakuwala, V.V. Kumar, S. Ramakrishna, S. Chandran, Sustainable recycling of polymers: a comprehensive review, Polymer Bulletin, (2024) 1-42.
[12] L. Liow, A. B. Clark, and N. Rojas, "Olympic: A modular, tend on driven prosthetic hand with novel finger and wrist coupling mechanisms," IEEE Robotics and Automation Letters, vol. 5, no. 2, 2020.
[13] Pratik Waghmare, "Design and Experimental Investigation of XY Compliant Mechanism for Precision Applications", ECS Transactions, 2022/4/24, Volume 107 Issue 1 Pages 4967. DOI 10.1149/10701.4967ecst
[14] Baviskar, D.D., Rao, A.S., Sollapur, S. et al. Development and testing of XY stage compliant mechanism. Int J Interact Des Manuf (2023). https://doi.org/10.1007/s12008-023-01612-1
[15] H. Zhou, A. Mohammadi, D. Oetomo, and G. Alici, "A novel monolithic soft robotic thumb for an anthropomorphic prosthetic hand," IEEE Robotics and Automation Letters, vol. 4, no. 2, pp. 602–609, 2019.
[16] M. D'Alonzo, F. Clemente, and C. Cipriani, "Vibrotactile stimulation promotes embodiment of an alien hand in amputees with phantom sensations," IEEE Trans. Neural Syst. Rehabil. Eng., vol. 23, no. 3, pp. 450–457, May 2015.
[17] Raut, P.P., Rao, A.S. et al. Investigation on the development and building of a voice coil actuator-driven XY micro-motion stage with dual-range capabilities. Int J Interact Des Manuf (2023). https://doi.org/10.1007/s12008-023-01665-2.

[18] L. Cao, A. Dolovich, W. J. Zhang, "On understanding of design problem formulation for compliant mechanisms through topology optimization," Mech. Sci, vol. 4, no. 2, pp. 357-369, 2013.
[19] B. Susanto, V.V. Kumar, L. Sean, M. Handayani, F. Triawan, Y.D. Rahmayanti, H. Ardianto, M.A. Muflikhun, Investigating Microstructural and Mechanical Behavior of DLP-Printed Nickel Microparticle Composites, Journal of Composites Science, 8 (2024) 247. https://doi.org/10.3390/jcs8070247
[20] Mathworks, "Global Optimization Toolbox User's Guide (R2015a)," pp.247-362, 2015.
[21] L. Cao, W. J. Zhang, "Integrated design of compliant mechanisms and embedded rotary actuators and bending actuators for motion generation," ASME IDETC, accepted, 2016.
[22] Y. Sun, Y. Liu, L. Xu, Y. Zou, A. Faragasso, and T. C. Lueth, "Automatic design of compliant surgical forceps with adaptive grasping functions," IEEE Robotics and Automation Letters, vol. 5, no. 2, pp. 1095–1102, 2020.
[23] Y. Sun, L. Xu, D. Zhang, and T. C. Lueth, "Automatic synthesis of compliant forceps for robot-assisted minimally invasive surgery," at – Automatisierungstechnik, vol. 68, no. 11, pp. 922–932, 2020.
[24] Venkate Gowda, C., Nagaraja, T.K., Yogesha, K.B. et al. Study on Structural Behavior of HVOF-Sprayed NiCr/Mo Coating. J. Inst. Eng. India Ser. D (2024). https://doi.org/10.1007/s40033-024-00641-8
[25] Y. Sun, Y. Liu, L. Xu, and T. C. Lueth, "Design of a disposable compliant medical forceps using topology optimization techniques," in 2019 IEEE International Conference on Robotics and Biomimetics (ROBIO), pp. 924–929, IEEE, 2019.